JEE Journal of Ecological Engineering

Journal of Ecological Engineering, 2026, 27(7), 12–27
https://doi.org/10.12911/22998993/216495
ISSN 2299–8993, License CC-BY 4.0

Received: 2025.12.05
Accepted: 2026.05.20
Published: 2026.06.01

Bond strength of fibrous recycled aggregate reinforced concrete

Nada Sahmi[1*], Eyad Sayhood[2], Nisreen Mohammed[3]

[1] Structural Engineering Department, College of Civil Engineering, University of Technology, Al Sana'ah street, Baghdad, Iraq
* Corresponding author's e-mail: nada.s.assi@uotechnology.edu.iq

ABSTRACT

Seven beam tests were conducted to examine the bond behavior of deformed bars in recycled aggregate concrete (RAC). Four different replacement ratios (R = 0%, 50%, 75%, and 100%) and volume fractions of steel fiber (Vf = 0.0%, 1.0%, 1.5%, and 2%) were taken into account as variable in this research. According to the test results, the bond degradation occurs when the replacement ratio of recycled concrete aggregate (RCA) rises. This degradation follows the same trend as the changes in the mechanical characteristics of recycled aggregate concrete when the replacement ratio increases. Furthermore, the use of steel fibers can enhance the bonding strength between steel reinforcement and steel fiber reinforced recycled aggregate concrete (SFRAC). It can also effectively reduce the formation of micro and macro cracks, leading to the failure of bond beam specimens in a ductile manner so obtain a greater level of confinement to the steel bar. The bond strength exhibited a negative correlation with the rise in the RCA replacement ratio. Conversely, it showed a positive correlation with the increase in the volume fraction of steel fiber. It is worth noting that the bond degradation due to poor mechanical properties prevented the improvement in bond behavior produced from utilizing steel fiber from keeping the maximum bond strength at the location where it was at the maximum bending moment; instead, it shifted towards the free end. Interestingly, this is an uncommon observation and comparatively unrecognized previously in beam tests to examine the bond behavior.

Keywords: recycled coarse aggregate (RCA), beam test, bond strength, bond stress–slip relationship, bond deterioration, steel fiber.

INTRODUCTION

In recent years, there has been a growing emphasis on expanding the use of recycled materials in the manufacturing of fresh concrete in order to minimize the environmental effects of concrete building (Dosho, 2007; Li, 2008). Recently, there has been significant interest in using coarse recycled concrete aggregate as a possible replacement for natural coarse aggregate (NCA). RCA is produced by processing construction and demolition waste. Nevertheless, the use of RCA concrete in structural projects has been delayed mainly due to concerns that concrete containing RCA may be of worse quality compared to concrete manufactured with NCA (Buck AD, 1973; Trindade et al, 2021). Previous research on recycled concrete aggregate (RCA) has examined various aspects, including the processing of demolished concrete, mixture design, and the physical, mechanical, and durability properties of the resulting materials. Comprehensive reviews of these studies were conducted by Nixon and Hansen (Nixon, 1978; Hansen, 1986). Their findings revealed that the mechanical performance of RCA-based concrete is generally lower than that of concrete made with natural coarse aggregates. To address these quality deficiencies, extensive research has been devoted to improving the characteristics of RAC through adjustments in particle gradation, enhancement of the interfacial transition zone, and the use of chemical admixtures. Recent studies consistently demonstrate that incorporating steel fibers as a reinforcing material effectively mitigates crack formation and propagation in concrete. Furthermore, steel fiber–reinforced recycled aggregate concrete (SFRAC) specimens typically exhibit a more ductile failure mode than RAC specimens

with equivalent mix proportions. The toughness, ductility, and splitting tensile strength of SFRAC have been shown to increase proportionally with the volume fraction of steel fibers (Vf). When the steel fiber content increases from 0.0% to 2.0%, the splitting tensile strength of SFRAC improves by approximately 84% (Ahmadi et al., 2017; Wang et al., 2019). Nevertheless, steel fibers do not demonstrate any substantial enhancement in the elastic modulus and compressive strength of SFRAC. Moreover, it is widely acknowledged that structural members constructed from SFRAC exhibit qualities that are equivalent to those of standard concrete members. Hence, the combination of RAC with fibers exhibits both technological validity and significant environmental advantages in engineering applications. Engineers interested in using recycled concrete aggregate for structural purposes to improve the sustainability of concrete construction would like to understand how RCA concrete behaves under different conditions compared to natural concrete aggregate and to what extent existing design codes, which were originally developed for NCA concrete, can be used to predict the strength and behavior of RCA concrete members in a conservative manner. Bond is a crucial characteristic of reinforced concrete that relates to the adhesion between the reinforcing steel and the surrounding concrete. This adhesion is responsible for the transmission of axial force between the two materials, guaranteeing strain compatibility and their composite action. The majority of research findings on the bond strength of RAC (Prince and Singh, 2014; Prince and Singh., 2015) suggest that the bond strength of RAC decreased with an increase in the replacement of recycled aggregate. While certain researchers (Kim et al, 2015; Guerra et al, 2014) have indicated that the bond strength of recycled aggregate concrete is comparable or even better than that of conventional concrete due to the enhanced integrity and mechanical properties of the concrete mass, it is generally observed that the bond strength of RAC is influenced by the ratio of recycled aggregate replacement (R). Steel fibers serve as a means of confinement, improving the toughness and bond performance of concrete, according to experimental results (Yazýcý and Arel, 2013; Huang et al, 2016). The tensile strength of the steel fiber reinforced concrete (SFRC) specimen increases by 7–16% as the volume fraction of steel fibers increases. although there have been several researches on the bond behavior between RAC and reinforcing steel, majority of these studies have focused on pullout specimens. However, there is a lack of examination of large-scale beams composed of recycled aggregate concrete. Losberg and Olsson (1979) determined that pullout tests are unsuitable for analyzing bond performance due to the variation in stress states between pullout tests, which involve additional confinement of concrete, and actual structures where splitting failure typically dominates., Losberg and Olsson concluded that pullout tests are not appropriate to study bond performance. To address this gap in the current state of knowledge, this study experimentally investigates the impact of various parameters on the relationship between bond stress-slip, In addition to the correlation between bonding stress-compressive strain in recycled aggregate reinforced concrete beams. The parameters considered include changes in the components of recycled aggregate concrete, specifically variations in recycled aggregate percentage and the amount of steel fibers present.

EXPERIMENTAL PROGRAM

Material

The coarse aggregates composed of natural coarse aggregates and recycled coarse aggregates as shown in Figure 1. The NCA consisted of crushed gravel with a maximum size of 12.5 mm. The recycled coarse aggregate was obtained by crushing wasted concrete using a jaw crusher. The original waste concrete had a compressive strength within the range of 27 to 38 MPa. To accommodate its high-water absorption rate, the RA was immersed in water for a duration and after this dried before being cast. Table 1 presents a detailed overview of the typical physical and chemical characteristics of both recycled aggregates (RA) and natural aggregates (NA) used in this study. Figure 2 illustrates the distribution of particle size for the recycled coarse aggregate. A local sand with a specific gravity of 2.62 was utilized as the natural fine aggregate (NFA). The test specimens were fabricated using Ordinary Portland cement type (I) that complies to the Iraqi standard NO.5/1984.

Bars with a diameter of 20 mm were utilized. The deformed bar has a yield strength about 500 MPa. A small, linear steel fibers were used in this experiment. Figure 3 and Table 2 display the

Figure 1. Several types of coarse aggregates that were utilized in this investigation (a) NCA, (b) RCA

properties of steel fibers. The impact of steel fiber on the characteristics of recycled aggregate concrete was examined and evaluated by including several percentages of volume fraction of steel fiber at 0%, 1%, 1.5%, and 2%.

Mixture proportion

The mixtures included N-F0, which had a compressive strength of 30 Mpa with natural aggregate R=0%, as well as R (100,75,50) % - F (0, 1, 1.5, 2) %. The specific compositions used throughout this project are outlined in Table 3. Given the high-water absorption, the RCAs were tested in their air-dried state. The doses of the polycarboxylate ether glinume 180 superplasticizer were modified in certain situations to achieve a similar level of workability**.** Thus, the workability of all mixtures was assessed soon after mixing, following the guidelines of ASTM C-143 test procedure, the slump test result, which conserved equal to 90±10mm for all mix by adjusting the quantity of admixture. The replacement ratio of RCA (R) was set at 0%, 50%, 75%, and 100%, which corresponds to the mass ratio of recycled coarse aggregate to total coarse aggregate.

Test specimens

Control specimen tests

This study aims to get an extensive understanding of the bond behavior of recycled aggregate concrete utilized in the examined beams. To achieve this, several experiments were conducted to experimentally examine the mechanical characteristics of recycled aggregate concrete. A whole of 84 cylindrical specimens with dimensions of 300 mm by 150 mm and 21 prisms measuring (100 × 100 × 400) mm (three for each mix) were created, cured, and subjected to tests accordance with specific guidelines for compressive strength ASTM C39/C39M, splitting tensile strength ASTM C496/C496M, flexural strength ASTM C78/C78M, and modulus of elasticity ASTM C469/C469M, after 28 days. In addition, the compressive strength at the day of the beam test.

Table 1. Characteristics of coarse aggregate in terms of its physical and chemical qualities

Type of aggregate	Absorption %	Specific gravity	Sulfate content
NA	0.55%	2.65	0.05%
RA	3.75%	2.55	0.085%

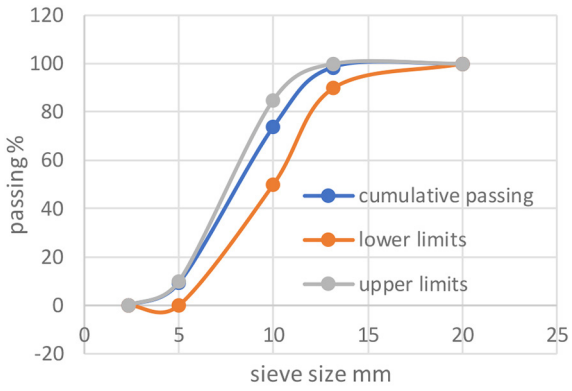

Figure 2. The grading of recycled coarse aggregate

Figure 3. Steel fibers

Beam test

The cross-sectional dimensions of the beam specimens are (200 × 300) mm, and their overall length is 2000 mm. Figure 4 depicts the configuration of the beam, the arrangement of

Table 2. Steel fiber properties

Summary of characteristics	Measurement of characteristics
Color	Auric
Diameter	0.2 mm
Density	7800 kg/m^3
characterization	straight
length/diameter (aspect ratio)	60
Ultimate tensile strength	>2850 MPa
length	12 mm

the experimental setup, and reinforcement details. Two notches measuring (100 × 80) mm were created across the width of the beam during the casting process. The purpose of these notches is for slip measurements can be taken by expose the tension bar. They were placed at the zone of maximum bending moment, which is located 250 mm beyond the interior surface of the supports at symmetrically positioned in beam specimens. In order to measure the slip at the free end, the tension bar was left exposed at both ends by two plastic pipes, were attached to the tension bar on both ends. The concrete beam was supported and subjected to two monotonic point loads provided using a hydraulic machine, the testing equipment was used to progressively increase the load at the far ends until the beam failed. The data logger recorded values of slip at the free ends and notches and the deflection in the mid-span, the maximum load capacity of the beams, the loads at which the first apparent cracks appeared, as well as both the concrete strain in the compression zone and the steel bar strain in the tension zone. These measurements were taken every second during the test. The transducers, including four concrete and steel strain gauges, load cell, as well as five linear differential transformers (LVDT), were used to measure these data.

Table 3. Key specifications of the steel fiber used in this study

No.	Mix symbol	fc´ MPa	Cement kg/m^3	NFA kg/m^3	NCA kg/m^3	RCA kg/m^3	SP l/m^3	Water l/m^3
1	N-F0	30	400	704	1056	0	0	180
2	R50-F0	**	400	704	528	528	0.7	180
3	R75-F0	**	400	704	264	792	0.73	180
4	R100-F0	**	400	704	0	1056	0.75	180
5	R100-F1	**	400	704	0	1056	1	180
6	R100-F1.5	**	400	704	0	1056	1.2	180
7	R100-F2	**	400	704	0	1056	1.4	180

Note: *the superplasticizer dose was adjusted to maintain the workability of all combinations while keeping the water content constant, **to be shown later.

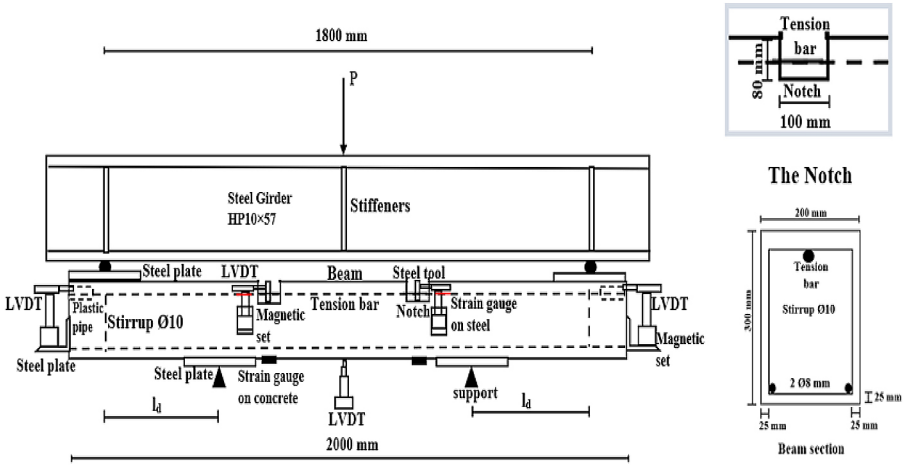

Figure 4. Illustrates the shape and arrangement of the beam, the experimental configuration and reinforcement details

Specimen's list

Table 4 provides comprehensive information on all the specimens used in this experiment. The image provides an explanation for the serial numbers assigned to the specimens. For instance, the code B1-N-F0 denotes the first beam, made of normal aggregate concrete, and without steel fiber reinforcement.

EXPERIMENTAL RESULTS AND DISCUSSION

The value of bond stress is calculated using the following formula, assuming a uniform distribution of bond stress along the anchoring length. In order to apply Equation 1, the steel stresses in the bars were measured throughout the test to the point of maximum bending, using both the measured strain in the steel bars (*εs)* and the modulus of elasticity of the steel bars (*Es*):

$$\mu = \frac{f_s d_b}{4 l_d} \quad (1)$$

where: μ – bonding stress (MPa); *fs* – steel reinforcing bars' stress (MPa); *db* – the diameter of the bar that has been developed (mm); l_d – bar's development length (mm).

Mechanical properties of RAC

The results of the compressive strength ($f'c$), splitting tensile strength (f_{cl}), flexural strength (f_r), and modulus of elasticity (Ec) are present in Table 5. In contrast to NAC, RAC consists of two types of ITZ (interfacial transition zone): the old ITZ between original aggregate and old mortar, as well as the new ITZ between original aggregate and new mortar, and between old mortar and new mortar, as seen in Figure 5. The modification of macroscopic mechanical characteristics of recycled aggregate concrete is deeply dependent on the composition of the material's microscopic structures and the physical and chemical changes occurring inside RAC. There are mainly two mechanisms:

- Degradation effect: The surface of recycled aggregate is bound to old cement mortar, resulting in a weak area of mechanical properties known as the interfacial transition zone between the new and old cement slurry (Verian et al., 2018). Additionally, the production process of recycled aggregate is prone to the formation of numerous micro-cracks under external force, which ultimately leads to a degradation of its mechanical properties (Omary et al., 2018).
- Strengthening effect: The higher porosity of recycled aggregate in RAC results in increasing water content and improves internal curing, which enhances the subsequent hydration reaction (Lei et al., 2018). Additionally, water can react with the remaining unhydrated cement paste that is stuck to the recycled aggregates' surface, accelerated the development of strength and improving the microstructural density (Kurad et al., 2017). Additionally, recycled aggregates' porosity allows for a stronger bond with the fresh mortar and absorbing more water from the interfacial transition zone (ITZ). This procedure successfully lowers the local water-to-cement ratio and increases the stiffness of particular areas. Furthermore, recycled aggregates' angular and rough surface texture promotes mechanical interlocking and interparticle friction, which enhances overall strength (Walraven, 1981).

During this experiment, it was observed that R% (the replacement rate of recycled coarse aggregate) falls within the range of 0–100%

Table 4. provides a description and detailed information on the beam specimen

Group	Identification	Mix	R.C %	Steel fiber Vf %	d_b mm	Cover mm	l_d mm
Reference group (Group 0)	B1-N-F0	M1-N-F0	0	0	20	40	250
Group 1	B2-R100%-F0	M2-R100-F0	100	0	20	40	250
	B3-R75%-F0	M3-R75-F0	75	0	20	40	250
	B4-R50%-F0	M4-R50-F0	50	0	20	40	250
Group 2	B5-R100%-F1	M5-R100-F1	100	1	20	40	250
	B6-R100%-F1.5	M6-R100-F1.5	100	1.5	20	40	250
	B7-R100%-F2	M7-R100-F2	100	2	20	40	250

Table 5. The mechanical properties of RAC

No.	Mix symbol	f´c (MPa) at 28 days	f´c (MPa) at test day	f_{ct} (MPa) at age 28 days	f_r (MPa) at age 28 days	E_c (MPa) at age 28 days
1	N-F0	30.18	34.54	4.80	5.13	26253
2	R50-F0	29.89	34.21	4.20	3.65	25449
3	R75-F0	29.21	33.43	3.55	3.04	24302
4	R100-F0	23.57	26.97	2.97	2.60	23419
5	R100-F1	31.24	33.67	4.22	3.72	26108
6	R100-F1.5	32.75	35.30	4.41	3.89	26664
7	R100-F2	33.19	35.77	4.50	3.99	26842

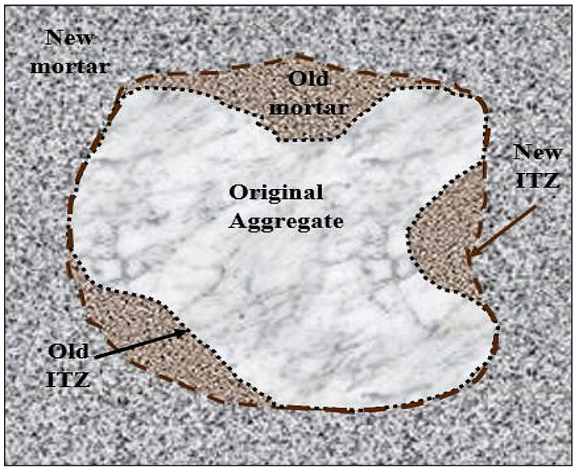

Figure 5. Representation of the interface transition zone (ITZ) in recycled aggregate concrete (RAC)

(N-F0, R50-F0, R75-F0 and R100-F0), the degradation impact becomes the main factor, leading to a decline in the compressive strength, splitting tensile strength, flexural strength, and modulus of elasticity of RAC about 21.90%, 38.13%, 31.58%, and 10.79% respectively as the replacement rate increases 0–100%. The impact used recycled coarse aggregate in concrete is not only reflected in the compressive strength value, but also in the failure modes, all samples exhibited a failure plane that was inclined, with varying angles of inclination for the macro-cracks, which impacted by R%, as seen in Figure 6. Figure 7 and 8 display mode failure of specimens for splitting tensile strength and flexural strength tests.

The steel fiber served as a bridge in the formation of macroscopic cracks, when steel fiber (SF) was added to the specimen, it not only reduced the expansion of primary cracks in the matrix during the early stage of crack development, but also improved the mechanical properties and enhanced the ability of SF to stop cracks from spreading. The results from Table 5, illustrate the impact of steel fiber ratios (Vf%) on mechanical properties, as well as Figures 9, 10, and 11, show failure mode for the compressive strength, splitting tensile strength, and flexural strength. When the volume fraction of steel fibers grows from 0.0% to 2.0%, the compressive strength, splitting tensile strength, flexural strength, and modulus of elasticity of steel fiber reinforced concrete (SFRAC) is approximately

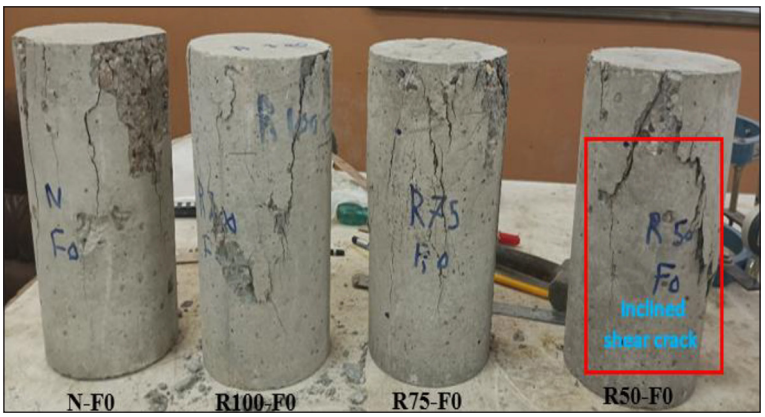

Figure 6. Cylindrical specimens after a compression test with different ratios of R%

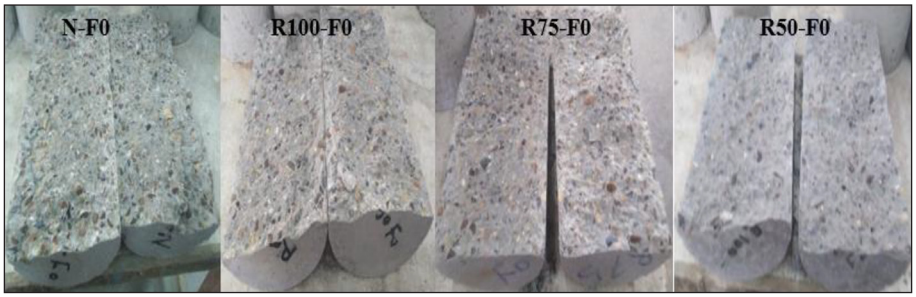

Figure 7. The failure mode of specimens for splitting tensile strength with various ratio of R%

Figure 8. The failure mode of specimens for flexural strength with various ratio of R%

improved by 32.62%, 51.46%, 53.46%, and 14.62% respectively. In addition, (as seen in Figures 9, 10, and 11), it has been demonstrated that the steel fiber reinforced recycled aggregate concrete specimens often exhibit a ductile failure when compared to RAC specimens with same mixture proportions. When comparing Figure 7, and 8 to Figure 10, and 11, the failure of the cylindrical and prism specimens with steel fiber was not divided into parts, it was prevented by the interlocking mechanism of the steel fibers, which acted as a medium to connect cracks and progress strength. Nevertheless, steel fibers do not demonstrate very high enhancement in the elastic modulus. This behavior may arise as a result of the test approach that was used. This technique determined the specimen's modulus of elasticity by applying 40% of its ultimate load during the elastic phase prior to cracking occurred. However, the steel perform successfully after cracks have formed. Thus, the estimation of the modulus of elasticity is mostly determined by the concrete compressive strength. Additionally, the steel fiber has a greater influence on the tensile characteristic-dependent properties than on other properties. Moreover, it is widely acknowledged that structural members constructed from SFRAC have similar qualities to those of standard concrete members. Consequently, the combination of RAC and fibers is technically feasible and offers significant environmental advantages in engineering applications. This study utilized steel fibers derived from novel steel, however, it is worth noting that fibers may also be manufactured from waste steel, so offering an additional means of mitigating waste concerns.

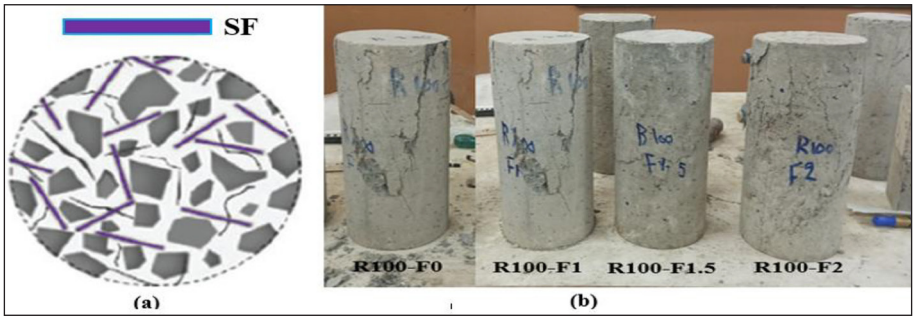

Figure 9. (a) Microstructural interaction mechanism of FRAC (Lin et al, 2023), (b) cylindrical specimens after a compression test with different ratios of steel fiber (Vf%)

Figure 10. The failure mode of splitting tensile strength specimens with R=100% and various ratio of Vf %

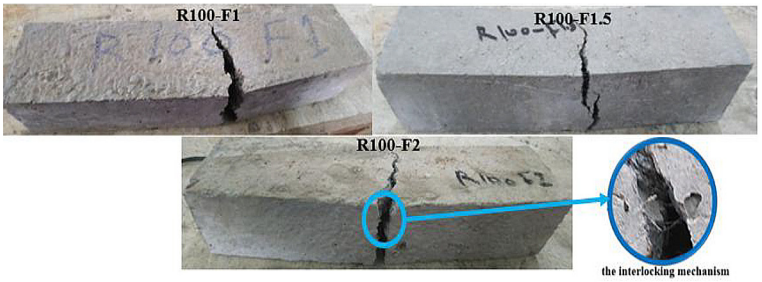

Figure 11. The failure mechanism of flexural strength specimens having R=100% and varying Vf % ratios

Bond behavior results based on beam tests

Seven large-scale reinforced concrete beams composed of recycled aggregates were constructed for this project. Each beam was 2000 mm in length and had a cross-section of 200 × 300 mm. The beams were cast, cured, and tested. The beams have been constructed in compliance with the ACI 318M-19 guidelines with the express purpose to undergo bond failure (anchorage loss). Subsequently, they were exposed to two monotonic loads until they reached the point of failure. The relative slippage between the reinforcing steel bars and the recycled aggregate concrete around them has been measured at two specific points. Furthermore, measurements have been conducted

Table 6. The findings of the experimental beam testing

Group	Beam	Pu (kN)	Δu (mm)	Pcr (kN)	Δcr (mm)	fs (Mpa)	Maximum slip at free end (mm)	Maximum slip at notch (mm)	Maximum compressive strain	Bond strength μf (Mpa)	Failure mode
G0	B1-N-F0	399.94	1.922	140.01	0.0393	263.90	0.483	0.657	0.000446	5.278	Bond Splitting failure
G1	B2-R100%-F0	358.49	1.841	119.49	0.0765	241.85	0.636	1.683	0.000544	4.837	Bond Splitting failure
	B3-R75%-F0	375.22	1.884	130.01	0.0263	249.50	0.582	1.399	0.000523	4.99	Bond Splitting failure
	B4-R50%-F0	384.74	1.886	135.95	0.0241	251.10	0.537	0.867	0.0005	5.022	Bond Splitting failure
G2	B5-R100%-F1	405.84	1.976	157.66	0.064	340.00	0.494	1.25	0.000646	6.8	Bond Splitting failure
	B6-R100%-F1.5	472.99	2.138	170.80	0.0414	367.50	0.4	1.16	0.00069	7.35	Bond Splitting failure
	B7-R100%-F2	501.64	2.233	226.23	0.0186	392.00	0.303	0.827	0.000705	7.84	Bond Splitting failure

for the concrete strain, steel strain, mid-span deflection, ultimate load capacity of beams (Pu), and load at first appearance of cracks (Pcr). Four LVDTs were used to measure the slipping, with two placed at the beam's free ends and the other two at the notches. In addition, four strain gauges were employed to measure the compressive strain in the concrete (εc), and tension strain in the steel bars (εs), while the upward mid-span deflections (Δu and Δcr) were recorded using an LVDT. Table 6 compiles the test results for all beams along with the effects of different factors on the main variables, which will be examined and discussed.

Parametric study

This study examines the impact of various parameters on the tested beams. To investigate these effects, The beams were categorized into two categories, along with a control beam. The parameters under consideration include adjustments in the components of recycled aggregate concrete, specifically changes in the percentage of recycled aggregate and the quantity of steel fibers used. The primary factors evaluated in this study included the maximum capacity of loading, first apparent crack load, upward deflection at mid span, slipping at notches, free end slipping, maximum zone strain in tension steel bars and compression side strain in concrete. All the impacts of the parameters are detailed below. It is important to highlight that in Table 6, For concrete, the majority of the documented values for compressive strain were less than 0.0039, which signifies the greatest strain for recycled aggregate concrete. The recorded values are inferior to the ultimate compressive strain of concrete, which is often not substantially influenced by an elevation in the replacement level of coarse RCA (Suryawanshim et al, 2018). Consequently, it may be stated that no beam experienced failure owing to concrete crushing.

Impact of recycled coarse aggregate ratio (R%)

This study aims to investigate the impact of varying ratios of recycled coarse aggregate on the relationship of bond stress-slip between recycled aggregate concrete and steel reinforcing bars. The experiment involved analyzing the results of three beams with recycled coarse aggregate ratios of 50%, 75%, and 100%, along with other significant factors. The beams in set number one were manufactured and tested beneath a two-point load. This set consists three beams labeled as B2-R100%-F0, B3-R75%-F0, and B4-R50%-F0. These beams were constructed using mixes M2-R100-F0, M3-R75-F0, and M4-R50-F0, with replacement ratios of 100%, 75%, and 50% respectively. Additionally, there is a control (reference) beam labeled as B1-N-F0 (M1-N-F0), which contains no replacement of natural coarse aggregate (0% replacement ratio).

The results of the analysis of these four beams are summarized in Table 6, while Figure 12 illustrates the beams that were studied, along with their corresponding patterns of cracking. According to the crack patterns seen in Figure 12, the tests show that bond splitting failure caused these four beams to collapse. The ultimate load capacity and the first cracking load exhibited reductions of 10.36% and 14.65% respectively, while the deflection at mid span reduced by 4.21% as the replacement ratio rose from 0–100%. These findings are illustrated in Figure 13a. When comparing the load-mid span deflection curve with the typical load-deflection curve of an RC beam failing in flexure (illustrated in Figure 14 (Campione et al, 2020)), it is evident that the curve is incomplete and consists only two stages: the uncracked concrete stage and the concrete cracked-elastic stresses stage. The ultimate-strength stage has not yet been reached due to bond failure.

A rising replacement rate of RCA has a negative impact on the bonding strength between the steel bars and the recycled aggregate concrete, resulting in a decrease of 8.35%. As mentioned before, the degradation impact becomes the main factor results a reduction in the mechanical characteristics of RAC as the replacement rate increases, leading to bond degradation. This has been confirmed by evidence from other literature sources (Prince and Singh, 2013; Xiao and Falkner, 2007) for pullout test specimens. However, it has a positive impact on the observed slipping at the free ends of the bars and notches. The slip at each location rose by ratios of 156.16% and 31.67% respectively as the replacement rate rose from 0% to 100%. Figures 13b and 13c display the bond stress - notch and free slip curves, respectively for the beam specimens at varying replacement ratios of RCA. Each bond stress-slip curve represents the bond behavior at distinct phases, namely micro slip, internal cracking, and pullout. These curves were incomplete, comprising just an ascending part due to a splitting failure. The observed difference between the NAC and RAC beam specimens is not substantial. Ultimately, the ultimate

compressive strain in the concrete increased as the replacement rate of RCA rose, with a growth rate of 21.97% as shown in Figure 13d. As the RCA% increases, the steel strain increases along the same linear path shown in Figure 13e for a same applied load. This is because the ultimate applied load decreases as the RCA% rises. Consequently, the average steel strain progress with respect to the applied load increment increases, which leads to failure with a smaller applied load. The ultimate strain in the steel bars decrease as the replacement rate of RCA increase, with an inclined rate of 8.35% as shown in Figure 13e. This decrease is due to the increase in replacement rate of RCA, this leads to a decrease in bond strength and ultimately causes rapid bond failure. This prevents the progress in tension strain in the steel bars. However, the change in bond stress relative to steel strain (slope) remains constant. The variation in replacement rate does not impact the slope, but it does have an influence on the steel strain. This is due to the yielding of bond stress to Equation 2, which was derived from Equation 1 with constant diameter and development length. The bond stress is strongly and directly affected by the diameter and development length in accordance with this equation. On the other hand, the ratios of recycled concrete aggregate and steel fiber have an indirect effect on bond stress. However, they do affect the steel strain, which in turn affects the bond. There is a linear positive correlation between the bond stress and steel strain (the steel has not yet reached the yield point). Ultimately, all the ultimate values of steel strain in Figure 13e are shown to be lower

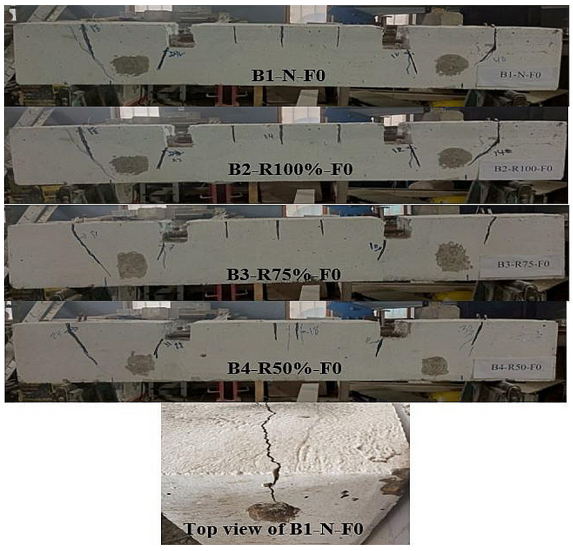

Figure 12. Examined beams from group 1, as well as the control beam (B1-N-F0)

than the yield steel strain which equal to 0.0025. This ensures that the failure is due to bond failure not the steel yielding. Figure 12 demonstrates that the main crack, which has the typical form of a bending crack near the support, this crack observed in NAC specimens were comparatively larger than those observed in RAC specimens. This discrepancy can be attributed to the fact that the fracture energy in NAC specimens is greater than that of those RAC.

$$\mu = \frac{d_b}{4\, l_d} f_s \rightarrow \mu = \frac{d_b E_s}{4\, l_d}\, \epsilon_s \qquad (2)$$

It is noteworthy that the main crack shifts from the position of maximum moment (load end) to the free end. This indicates that the maximum bond stress shifts towards the free end as bond degradation increases. This conclusion conforms with the findings of (Liu et al., 2020; Ma et al., 2017) for pullout specimens and (Zhao et al., 2013) for beam specimens with various reason of bond degradation (freeze-thaw and bar corrosion respectively). Their findings indicated that the distribution curves of bond stress at various relative locations for the same slip demonstrated that the specimens' middle section (between free and notch ends) displayed the maximum bond stress. The specimens' middle section demonstrates a higher degree of confinement, leading to improved bonding, which is a logical outcome. Therefore, the utilization of recycled aggregate concrete causes a degradation in the bond (even utilize traditional concrete with relatively low mechanical properties and low embedment length as reference beam), causing a shift in the location of maximum bond stress towards the free end. As a result, greater anchoring length is required under the same load. Furthermore, the scientists must fabricate additional beam specimens and affixed strain gauges to the steel bars in order to expand upon this investigation.

Impact of the ratio of steel fibers (Vf %)

This study examines the impact of the ratio of steel fibers on the bonding behavior and slipping between steel reinforcing bars and the surround recycled aggregate concrete, In addition to the bonding stress-slip relationships. Additionally, it investigates the compressive strain of concrete, ultimate load capacity, and mid-span deflection. The experiment involved investigating the effects of different volumetric ratios of steel fibers in four beams. The beams were labeled as B5-R100%-F1,

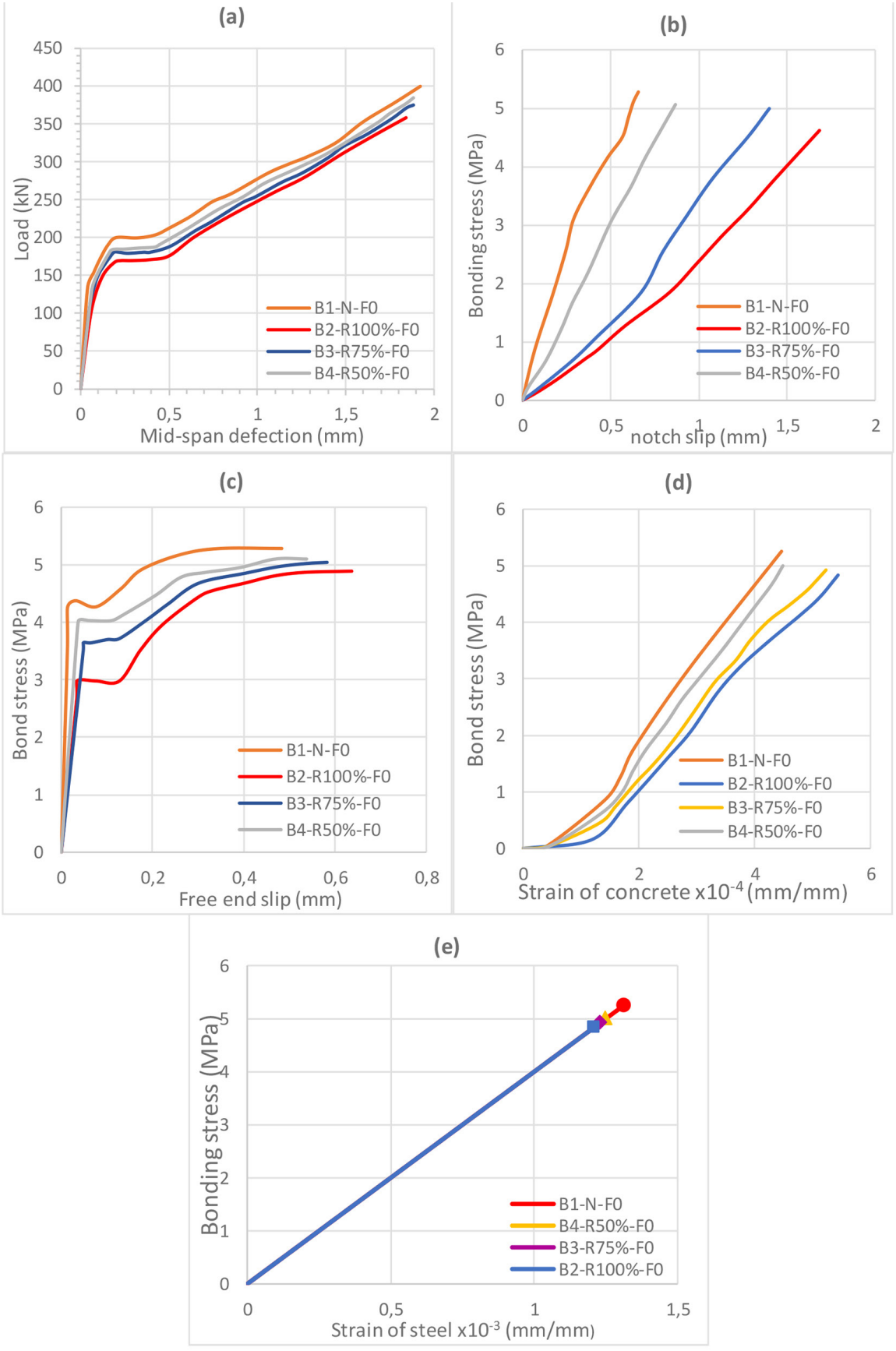

Figure 13. a comparison of correlations for beams with varying R%: (a) mid span load-deflection curve, (b) bonding stress–notch slipping relationship, (c) Bond stress–free end slip relationship, (d) bonding stress-concrete strain relationship, (e) bond stress-steel strain relationship

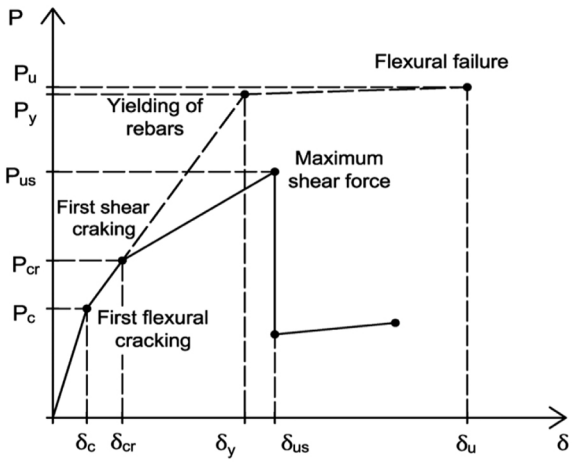

Figure 14. The load-deflection curve of a reinforced concrete beam that fails either due to flexure or shear (Campione et al., 2020)

B6-R100%-F1.5, and B7-R100%-F2, representing group number 2. The steel fibers volumetric ratios in these beams were 1%, 1.5%, and 2%, respectively. The mixes used for these beams were M5-R100-F1, M6-R100-F1.5, and M7-R100-F2. Figure 15 displays the beams that were examined and exhibits the patterns of cracks. These cracks suggest that all of the beams failed due to bond splitting failure, anchoring loss. In addition, the beam B2-R100%-F0 (M2-R100-F0) utilizes a steel fiber volumetric ratio of 0% for comparison.

The test outcomes for these beams, as detailed in Table 6, indicate that the peak load capacity and the load at which the first crack occurred grew by 39.93% and 89.32% respectively, with the steel fibers' volumetric ratio rising from 0% to 2%. Additionally, the mid span deflection rose by 21.29% (load -mid span deflection still incomplete). This is illustrated in Figure 16a. The inclusion of steel fiber (SF) has been seen to effectively avoid immediate splitting of bond beam specimens, postpone internal cracking of concrete, and maintain a high bearing capacity for fiber reinforced recycled aggregate concrete (FRAC) beams. During the experiment, the bridging action of SF may effectively limit the formation of cracks in RAC and cause the FRAC beam specimens to collapse in their ductile state. The bonding strength between the steel bars and the recycled aggregate concrete exhibits a significant increase of 62.08%. In contrast, slipping at the free ends of the bars and notches decreases by 52.35% and 50.86% respectively, when the steel fibers content changes from 0% to 2%. This is illustrated in Figure 16b and Figure 16c. The bond-slip (notch and free) curve of the bond beam specimens remains incomplete despite the incorporation of steel fiber. The bond stress increases throughout the ascending stage as the Vf% increases, in comparison to the B2-R100%-F0 beam specimen. Moreover, it has been observed that the slope of the first part of the ascending branches is always approximately the same in all instances, and the relationship between bond stress and slip stays linear. The resistance of the bond mostly depends on the chemical adhesion and friction at this stage, and the inclusion of SF does not significantly affect the stiffness of the bond. The ultimate compressive strain in concrete exhibited a proportional increase of 29.59% when the steel fibers' volumetric ratio become from 0% to 2%, as shown in Figure 16d. A rise in Vf% causes the steel strain to decrease on the same linear path for Figure 16e for a same applied load, as the Vf % rises the average of steel strain progress decrease. Figure 16e demonstrates that the ultimate strain in steel increase when the steel fibers' volumetric ratio changed from 0% to 2% about 62.08%, as well as, illustrate the same observations was previously noticed and discuss in Figure 13e, with a notable increase in steel strain resulting from improvement bond behavior. However, from an engineering perspective, the Vf ≈ 1.0–1.5% represents an optimal range, offering a favorable balance between bond enhancement, ductility improvement, and practical workability. Any Increasing Vf beyond this range may

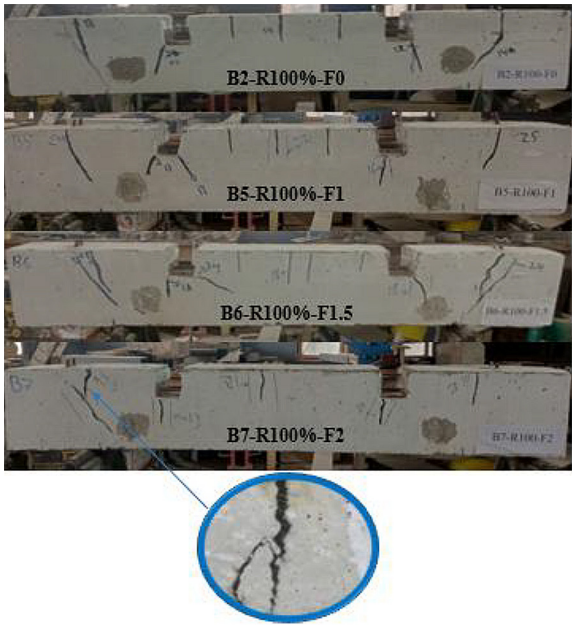

Figure 15. Examined beams from group 2, as well as the B2-R100%-F0

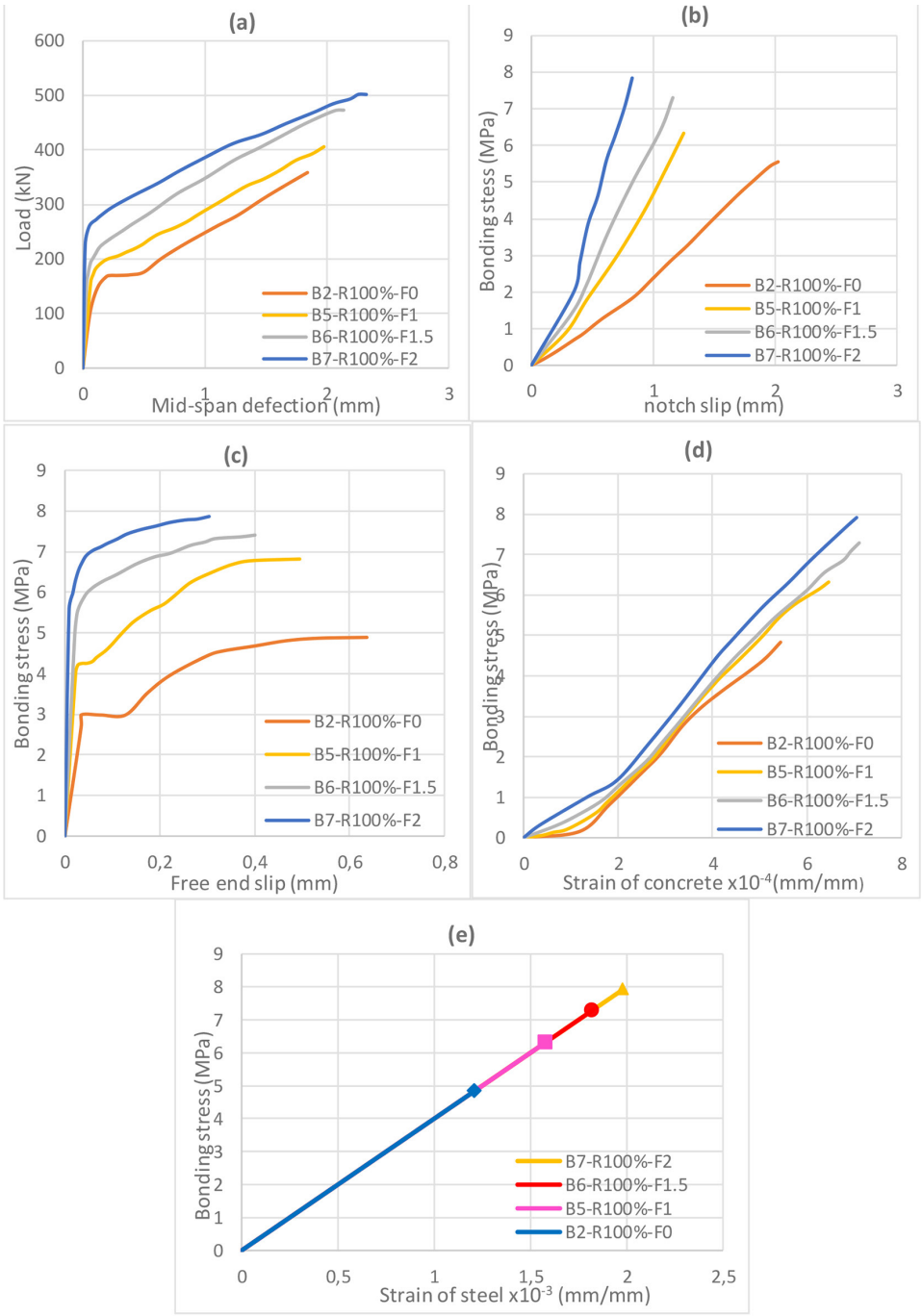

Figure 16. A comparison of correlations for beams with varying Vf%: (a) mid span load-deflection curve, (b) bonding stress–notch slipping relationship, (c) bonding stress–free end slipping relationship, (d) bonding stress-concrete strain relationship, e) bonding stress-steel strain relationship

still improve bond performance under controlled laboratory conditions, but the marginal structural benefit may not justify the practical drawbacks in field applications. As demonstrated in Figure 15, the position of the highest bond stress is still shifting towards the free end, even when utilizing steel fiber and its ability to enhance bond behavior. In order to address the deterioration of the bond, additional factors are required to enhance the bond's behavior. The presence of steel fiber in the beams significantly reduces the crack width compared to the B2-R100%-F0 beam, due to the bridge mechanism provided by the steel fiber.

The experimentally observed shift of peak bond stress toward the free end further indicates that, in RAC, anchorage length requirements may be underestimated if conventional uniform bond stress assumptions are used. This highlights the

need for caution and potentially longer development lengths when high RCA contents are employed. A larger test matrix would be required to develop design equations or reduction factors suitable for direct code implementation. The present work should therefore be interpreted as a mechanistic and exploratory experimental study, forming a basis for future expanded research.

Furthermore, comprehensive cyclic and fatigue testing is necessary to quantify degradation rates, stiffness reduction, and energy dissipation, and is recommended as a key focus for future research.

CONCLUSIONS

Based on the results of the beam tests and the control specimens testing, the following observations and conclusions may be concluded from this study. The mechanical properties are negatively correlated with the ratio of recycled concrete coarse aggregate R%. The test findings demonstrated a notable decline in the compressive strength, splitting tensile strength, flexural strength, and modulus of elasticity of RAC as the replacement rate rose from 0% to 100%. Nevertheless, the mechanical characteristics of steel fiber recycled aggregate concrete SFRAC, are positively correlated with the steel fiber. The use of SF can successfully prevent the formation of both micro and macro cracks, leading to the failure of the specimens in a ductile manner. Moreover, the steel fiber exhibits a more significant impact on attributes that depend on tensile characteristics compared to other properties.

Similar to the mechanical characteristics behavior of RAC, bond deterioration occurred as the replacement ratio increased. The bond strength of the RAC specimen is reduced by 8.35% compared to traditional concrete occurred as the replacement ratio increased from 0–100%. The decrease also encompasses the maximum load capacity, the first cracking load, the mid span deflection, and ultimate steel strain. The replacement ratio positively affects the slipping seen at both free ends and notches, as well as, compressive strain in concrete.

The bonding strength between the recycled aggregate concrete and the steel bars demonstrates a notable increase of 62.08%. Additionally, the maximum load capacity, first crack load, upward deflection at mid span, compressive strain in concrete, and ultimate steel strain all demonstrate a proportional increase when the steel fibers' volumetric ratio changes from 0% to 2%. On the other hand, the slipping at the free ends and notches experiences a reduction of 50.86% and 52.35% correspondingly, when the steel fibers content varies from 0% to 2%. Additionally, the bond failure mechanism of SFRAC beam specimens was ductile (similar to control specimens). This was due to the fact that the cracks in SFRAC did not rapidly enlarge upon reaching the point of creaking strength. The observed trend may be attributed to the proper utilization of SF, which successfully stops the development and expansion of both micro and macro cracks. As a result, the steel rebar experiences a higher degree of confinement.

The primary crack moves from the location of highest moment (load end) to the free end. This shows that when bond deterioration occurs, the maximum bond stress moves towards the free end. In order to explain this phenomenon, it can be observed that the central section located between the load end and the free end of the specimens, exhibits a greater degree of bond stiffness when compared to the load end and free end sections. Although steel fiber is utilized to enhance bond behavior, the position of the highest bond stress still shifts closer to the free end. In order to fix the deterioration of the bond, additional components are required to enhance the bond's performance like the diameter and development length of steel bar.

Acknowledgements

The authors are grateful for the financial support towards this research by the College of Civil Engineering, University of Technology, Baghdad / Iraq. Postgraduate Research Grant (PGRG) No.ع.م.م/890/29/10/2020.

REFERENCES

1. ACI Committee 318. ACI 318-19 Building Code Requirements for Structural Concrete (ACI 318-19) and Commentary (ACI 318R-19). American Concrete Institute.
2. Ahmadi, M., Farzin, S., Hassani, A., Motamedi, M. (2017). Mechanical properties of the concrete containing recycled fibers and aggregates. *Construction and Building Materials. 144*, 392–398. https://doi.org/10.1016/j.conbuildmat.2017.03.215
3. ASTM C39/C39M - 15a, Standard Test Method

for Compressive Strength of Cylindrical Concrete Specimens, Vol. 04.02, 2015, 7p.

4. ASTM C469/C469M – 14, Standard Test Method for Static Modulus of Elasticity and Poisson's Ratio of Concrete in Compression, Vol. 04.02, 2014, 5p.
5. ASTM C496/C496M - 11, Standard Test Method for Splitting Tensile Strength of Cylindrical Concrete Specimens, Vol. 04.02, 2011, 5p.
6. ASTM C78/C78M - 15a, Standard Test Method for Flexural Strength of Concrete (Using Simple Beam with Third-Point Loading), Vol. 04.02, 2015, 4p.
7. Buck AD. (1973). Recycled concrete. Highway Research Record. *Washington: Highway Research Board*, p. 1–8. http://dx.doi.org/10.3151/jact.5.3
8. Campione, G., Ferrotto, M. F., Papia, M. (2020). Flexural Response of RC Beams Failing in Shear. *Design and Construction*, © ASCE, 25(4), 04020028. https://doi.org/10.1061/(ASCE)SC.1943-5576.0000507
9. Domingo-Cabo, A., Lázaro, C., López-Gayarre, F., Serrano-López, M.A., Serna, P., Castaño-Tabares, J.O. (2009). Creep and shrinkage of recycled aggregate concrete. *Construction and Building Materials*, *23*(7), 2545–2553. https://doi.org/10.1016/j.conbuildmat.2009.02.018
10. Dosho Y. (2007). Development of a sustainable concrete waste recycling system – application of recycled aggregate concrete produced by aggregate replacing method. *Journal of Advanced Concrete Technology,5*(1), 27–42. https://doi.org/10.3151/jact.5.27
11. Guerra, M., Ceia, F., de Brito, J., Julio, E. (2014). Anchorage of steel rebars to recycled aggregate concrete. *Construction & Building Materials, 72*, 113–123. https://doi.org/10.1016/j.conbuildmat.2014.08.081
12. Hansen, T.C. (1986). Recycled aggregates and recycled aggregate concrete second state-of-the-art report developments 1945–1985. *Materials and Structures, 19*, 201–246. http://dx.doi.org/10.1007/BF02472036
13. Huang, L., Chi, Y., Xu, L.H., Chen, P., Zhang, A. (2016). Local bond performance of rebar embedded in steel-polypropylene hybrid fiber reinforced concrete under monotonic and cyclic loading, *Construction & Building Materials*, *103*, 77–92. https://doi.org/10.1016/j.conbuildmat.2015.11.040
14. Iraqi Specification, No. 5/1984, "Portland Cement".
15. Kim, S. W., Yun, H. D., Park, W. S., Jang, Y.-I. (2015). Bond Strength Prediction for Deformed Steel Rebar Embedded in Recycled Coarse Aggregate Concrete. *Materials & Design, 83*(9), 257–269. https://doi.org/10.1016/j.matdes.2015.06.008
16. Kurad, R., Silvestre, J.D., de Brito, J., Ahmed, H. (2017). Effect of incorporation of high volume of recycled concrete aggregates and fly ash on the strength and global warming potential of concrete. *Journal of Cleaner Production*, *166*(4), 485–502. https://doi.org/10.1016/j.jclepro.2017.07.236
17. Lei, B., Li, Z.X., Zou, J., Xiong, J. (2018). Experiment on durability of recycled concrete under coupling multi-factors of load and corrosion freeze-thaw. *Nongye Gongcheng Xuebao/Transactions of the Chinese Society of Agricultural Engineering (Trans. CSAE), 34*(20), 169–174. https://doi.org/10.11975/j.issn.1002-6819.2018.20.021
18. Li X. (2008). Recycling and reuse of waste concrete in China Part 1. Material behavior of recycled aggregate concrete. *Resources, Conservation and Recycling*, *53,* 36–44. http://dx.doi.org/10.1016/j.resconrec.2008.09.006
19. Lin, G., Liu, K., Chen, Y., Ji, Y., Jiang, R. (2023). Experimental Investigation on Compressive Properties of Fiber Recycled Aggregate Concrete. *Journal of Renewable Materials*, *11*(11), 3957–3975. https://doi.org/10.32604/jrm.2023.028290
20. Liu, K., Yan, J., Meng, X., Zou, C. (2020). Bond behavior between deformed steel bars and recycled aggregate concrete after freeze thaw cycles. *Construction and Building Materials*, *232*(6), 117236. https://doi.org/10.1016/j.conbuildmat.2019.117236
21. Losberg, A., and Olsson, P.-A., (1979). Bond failure of deformed reinforcing bars based on the longitudinal splitting effect of the bars. *ACI JOURNAL, Proceedings 76*(1), 5–18.
22. Ma, Y., Guo, Z., Wang, L. et al. (2017). Experimental investigation of corrosion effect on bond behavior between reinforcing bar and concrete. *Construction and Building Materials*, *152*, 240–249. https://doi.org/10.1016/j.conbuildmat.2017.06.169
23. Nixon, PJ. (1978). Recycled concrete as an aggregate for concrete – a review. *Materials and Structures,11*(65), 371– 378. https://doi.org/10.1007/BF02473878
24. Omary, S., Ghorbel, E., Wardeh, G., Nguyen, M.D. (2018). Mix design and recycled aggregates effects on the concrete's properties. *International Journal of Civil Engineering*, *16*(2), 973–992. https://doi.org/10.1007/s40999-017-0247-y
25. Prince, M. J. R., Singh, B. (2013). Bond behavior of deformed steel bars embedded in recycled aggregate concrete. *Construction & Building Materials, 49*(6), 852–862. https://doi.org/10.1016/j.conbuildmat.2013.08.031
26. Prince, M. J. R., Singh, B. (2014). Bond behavior of normal- and high-strength recycled aggregate concrete. *Structural Concrete*, *16*(1), 56–70. https://doi.org/10.1002/suco.201300101
27. Prince, M. J. R., Singh, B. (2015). Bond strength of deformed steel bars in high-strength recycled aggregate concrete. *Materials and Structures, 48*(12), 3913–3928.

https://doi.org/10.1617/s11527-014-0452-y

28. Suryawanshi, S., Singh, B., Bhargava, P. (2018). Equation for stress–strain relationship of recycled aggregate concrete in axial compression. *Magazine of Concrete Research*, *70*(4), 163–171. https://doi.org/10.1680/jmacr.16.00108
29. Trindade, J., Garcia, S.L., Torre, H. (2021). Shear Strength of concrete with recycled aggregates reinforced with steel fibers. *ACI Materials Journal 118*(5), 185-198. https://doi.org/10.14359/51732984
30. Verian, K.P., Ashraf, W., Cao, Y. (2018). Properties of recycled concrete aggregate and their influence in new concrete production. *Resources, Conservation and Recycling*, *133*, 30–49. https://doi.org/10.1016/j.resconrec.2018.02.005
31. Walraven, J.C. (1981). Fundamental analysis of aggregate interlock. *Journal of the Structural Division. ASCE*, *107*(11), 2245. https://doi.org/10.1061/JSDEAG.0005820
32. Wang, X.H., Zhang, S.R., Wang, C., Cao, K.L., Wei, P.Y., Wang, J.X. (2019). Effect of steel fibers on the compressive and splitting-tensile behaviors of cellular concrete with millimeter-size pores. *Construction and Building Materials. 221*, 60–73. https://doi.org/10.1016/j.conbuildmat.2019.06.069
33. Xiao J., Falkner H. (2007). Bond behavior between recycled aggregate concrete and steel rebars. *Construction and Building Materials, 21,* 395–401. https://doi.org/10.1016/j.conbuildmat.2005.08.008
34. Yazýcý, S., Arel, H.S. (2013). The effect of steel fiber on the bond between concrete and deformed steel bar in SFRCs. *Construction & Building Materials*, *40*, 299–305. https://doi.org/10.1016/j.conbuildmat.2012.09.098
35. Zhao, Y., Lin, H., Wu, K., Jin, W. (2013). Bond behavior of normal/ recycled concrete and corroded steel bars. *Construction & Building Materials*, *48*, 348–359. https://doi.org/10.1016/j.conbuildmat.2013.06.091